Available online at www.sciencedirect.com
ScienceDirect
Journal of the European Ceramic Society 27 (2007) 4007–4010
www.elsevier.com/locate/jeurceramsoc

Characterization of ferroelectrics by thermal wave methods

A.A. Movchikova [a,*], G. Suchaneck [b], O.V. Malyshkina [a], G. Gerlach [b]

[a] *Tver State University, Department of Ferroelectric and Piezoelectric Physics, Sadovij per. 35, 170002 Tver, Russia*
[b] *Technische Universität Dresden, Institut für Festkörperelektronik, Helmholtzstrasse 10, 01062 Dresden, Germany*

Available online 2 April 2007

Abstract

In this work, pyroelectric spatial profiles of SBN crystals, $BaTi_{1-x}Sn_xO_3$ ceramics, and $Pb(Zr,Ti)O_3$ thin films were determined from the pyroelectric current spectrum caused by the interaction of thermal waves with the internal electric field and the unknown polarization distribution. For sinusoidal modulation, the pyroelectric current frequency dependence up to 10 MHz and phase shift between pyroelectric current and heat flux were analyzed to reconstruct the polarization distribution by solution of the Fredholm integral equation and by a Tikhonov regularization method for stable MATLAB numerical solutions. For the dynamic method with rectangular modulation, an approximate pyroelectric response in dependence on penetration depth was calculated. In this case, low modulation frequencies are required for the investigation of deep regions. Digital methods of signal processing were used to enable experiments below 1 Hz.

Keywords: Ferroelectric properties; Perovskites; Pyroelectric spectroscopy

1. Introduction

Thermal waves techniques for non-destructive probing of electric field and polarization profiles in dielectric materials are known for almost half a century.[1–14] In the so-called laser intensity modulation method (LIMM),[8] the energy of a modulated laser beam absorbed in the sample generates well defined thermal waves, which propagate in the sample and cause local changes in temperature, thermoelastic strains, pyroelectric response, etc. By travelling through the sample, the thermal wave with a wave vector is both attenuated and retarded in phase. Thus, the depth resolution of the LIMM techniques is limited by the modulation frequency of the light beam. The spatial resolution is non-uniform with a maximum near the thermally excited electrode at the penetration depth of the thermal wave:

$$d_D = \sqrt{\frac{2D}{\omega}}, \tag{1}$$

where ω is the circular frequency of modulation and D is the thermal diffusivity. It rapidly decrease within the sample.[10,13,14] Considering a thermal diffusivity of 0.5 mm^2/s, the penetration depths of the thermal wave amount to 400 nm to 400 μm for frequencies between 1 MHz and 1 Hz, respectively. Therefore, one challenge for investigating the near surface region is to increase the modulation frequency of the incident radiation which generates the travelling thermal wave within the sample. Another challenge is the increase of the thermal wave penetration depth at frequencies below 1 Hz to enable the polarization profiling of ceramic and single crystal samples. In the latter case, rectangular pulses could be applied since they comprise a wide frequency range which upper bound is given by one-half of the analog–digital converter sampling frequency.

Assuming that the radius of the thermally excited top electrode is much larger than the sample thickness, the transient temperature distribution across the sample thickness is a one-dimensional problem. The complex pyroelectric current yields under short-circuit conditions to[9]:

$$I(\omega, t) = I_p \cdot e^{j\omega t} = \frac{A_S}{d} \int_0^d r(z) \frac{\partial}{\partial t} \underline{\hat{T}}(\omega, z, t)\, dz, \tag{2}$$

where I_p is the complex amplitude of the pyroelectric current, z the depth coordinate, t the time, $\underline{T}$ the complex amplitude of the temperature, A_S the heated area of the sample, d the ferroelectric film thickness and $r(z)$ is the response function. The pyroelectric response function is determined both by the pyroelectric coefficient $p(z)$ and the internal electric field E_{int}, generated in a short-circuited sample ($E = 0$ at electrode surfaces) due to space

* Corresponding author. Tel.: +7 9038022387.
E-mail address: alena-ftf@mail.ru (A.A. Movchikova).

0955-2219/$ – see front matter © 2007 Elsevier Ltd. All rights reserved.
doi:10.1016/j.jeurceramsoc.2007.02.083

charges, and the depolarization field:

$$r(z) = \alpha_P P(z) - (\alpha_z - \alpha_\varepsilon)\varepsilon\varepsilon_0 E_{\text{int}}(z) = p(z) - (\alpha_z - \alpha_\varepsilon) \cdot \varepsilon\varepsilon_0 E_{\text{int}}(z), \quad (3)$$

where α_p, α_z and α_ε are relative temperature coefficients with $\alpha_X = 1/X\,\mathrm{d}X/\mathrm{d}T$. Considering either a thermally isolated or thermally coupled one-layer system, Eq. (2) may be solved analytically by means of the Mellin transform.[11] If the sample is assumed as a semi-infinite solid, the temperature distribution is given by[12,13]:

$$T(z,t) = \frac{(1-i)\cdot\Phi_0 d_{\text{D}}}{2k}\exp\left(-\frac{(1-i)\cdot z}{d_{\text{D}}}\right), \quad (4)$$

where Φ_0 is the absorbed heat flux and k is the thermal conductivity.

Usually, thin film samples are multilayer systems where thermal mass of the substrate or even a supporting membrane with a thickness comparable to that of the ferroelectric thin film have to be taken into account. Here, analytic solutions of the thermal problem become cumbersome. A numerical procedure for solution of the thermal problem and reconstruction of the pyroelectric response function is described in detail.[11] It is based on MATLAB software containing algorithms for the inverse solution of the appropriate Fredholm integral equation and a Tikhonov regularization.[6,11]

In the case of both-side electroded ceramics, probed by thermal waves with a penetration depth much smaller than the sample thickness, an approximate profile of the pyroelectric coefficient is given by[9]:

$$p(d_{\text{D}}) = \frac{c\rho d}{\Phi_0 A_{\text{S}}}[\text{Re}(I_{\text{p}}(\omega)) - Im(I_{\text{p}}(\omega))], \quad (5)$$

where c is the specific heat of the ceramics, ρ the density and $\text{Re}(I_{\text{p}}(\omega))$ and $\text{Im}(I_{\text{p}}(\omega))$ are the real and imaginary part of the pyroelectric current, respectively.

In the case of a periodic train of rectangular light pulses, higher harmonics appear due to the Fourier series representation. The distribution of the temperature increment for $d > d_{\text{D}}$ in a thermally isolated sample is then given by[7]:

$$\Delta T(z,t) = \frac{2\Phi_0}{k}\cdot a\cdot\sum_{n=1}^{\infty}\frac{\sin n\pi a}{n\pi a} \cdot\frac{\cosh[(1+i)(d-z)/d_n]\cdot d_n}{(1+i)\cdot\sinh[(1+i)d/d_n]}\cdot\exp(in\omega\cdot t), \quad (6)$$

where $\omega = 2\pi/T$ is the fundamental frequency of the repeating pulse pattern, $a = \tau_{\text{P}}/T$ the duty factor for a pulse time τ_{P}, and $d_n = d_{\text{D}}/\sqrt{n}$ is the penetration depth due to higher harmonics of the thermal wave. In this case, the pyroelectric coefficient at the thermal wave penetration depth is may be approximately determined by[15]:

$$p(d_{\text{D}}) = \frac{I(\omega)\cdot k\pi}{A_{\text{S}}\Phi_0}\frac{1}{\sum_{n=0}^{\infty}[\sin^2(a\pi\cdot n)/a\pi\cdot n^2]d_{\text{D}}\omega\cdot[1-\exp(-(1+i)\sqrt{n})]} \quad (7)$$

In this work, both the dynamic method with rectangular modulation and the LIMM method with sinusoidal modulation were used to evaluate pyroelectric spatial profiles of undoped and doped SBN crystals, $BaTi_{1-x}Sn_xO_3$ ceramics, and $Pb(Zr,Ti)O_3$ thin films.

2. Experimental

$Pb(Zr,Ti)O_3$ thin films were deposited by multi-target reactive sputtering at TU Dresden.[16] $BaTi_{1-x}Sn_xO_3$ functional ceramics with a gradient of $0.075 \le x \le 0.15$ were synthesized at Martin Luther University Halle (Germany).[17] The tin gradient was formed by successive pressing of granulated powder with different Sn content and a subsequent sintering for one hour at 1400 °C under an uniaxial pressure of about 1 kPa. Al electrodes were evaporated onto both sample sides. Poling is performed at 20 kV/cm by applying a positive dc voltage to either of the electrodes. Undoped $(Sr,Ba)Nb_2O_6$ (SBN) crystals and doped with Cr or Ce ones were provided by Prof. S. Kapphan (University of Osnabrueck, Germany). The domain structure of the crystals was modified by an alternative electric field treatment (AEFT) at a frequency of 50 Hz with an amplitude of about 3 kV/cm.

The pyroelectric current spectrum generated by a sinusoidal modulated semiconductor laser with a power of 10 mW at a wavelength of 1.55 μm, modulated with frequencies up to 10 MHz, was transformed into a voltage by a current–voltage converter. Amplitude and phase were determined by an impedance–phase analyzer. The current spectra were corrected by reference measurements with an InGaAs photo-diode. The numerical reconstruction of the pyroelectric coefficient profile was based on an eight-layer thermal model.[11]

For square wave modulation, the on–off cycle of an IR-photodiode (λ = 930–960 nm) was controlled by a wave function generator G6-28 connected in series with a power amplifier. The pyroelectric current was converted to voltage by an operational amplifier K140UD8 with conversion coefficient of 25 V/μA at a bandwidth of 100 Hz or an operational amplifier OP297 with conversion coefficients of 250 V/μA and 2500 V/μA at bandwidths of 1000 and 100 Hz, respectively. Signal sampling was performed by a 12-bit analog–digital converter LA-70M4 at a sampling frequency of 13 kHz. Digital signal processing methods enables experiments below 1 Hz. In this case, the lower frequency limit was determined by the condition that d_{D} should not exceed the sample thickness.

3. Results and discussion

Fig. 1a illustrates the pyroelectric current spectrum of poled $Pb(Pb_{0.31}Zr_{0.28}Ti_{0.41})O_3$ thin films with a thickness of 600 nm deposited onto platinized silicon wafers as described.[16] The pyroelectric coefficient profile (Fig. 1b) was reconstructed following.[11] The as-grown film shows a small self-polarization corresponding to an averaged pyroelectric coefficient of about 2 nC/cm^2 K. After poling by applying a dc voltage of 15 V to

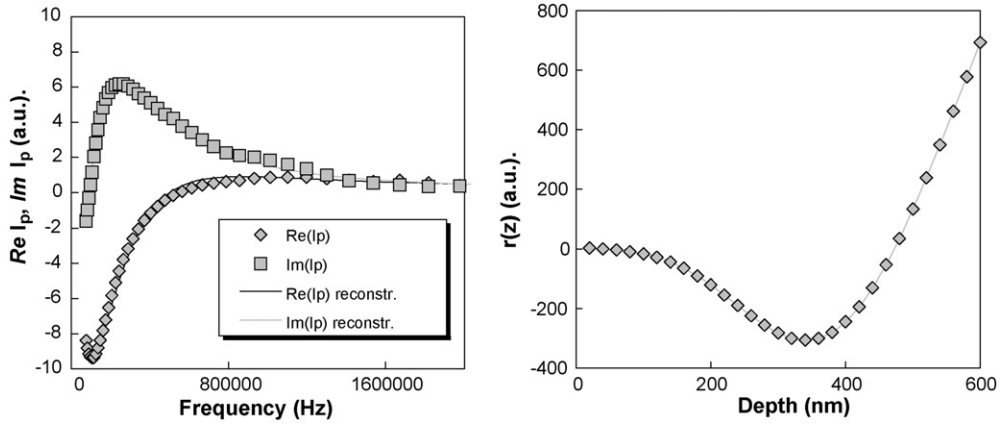

Fig. 1. Pyroelectric current spectrum (a) and pyroelectric coefficient profile (b) of $Pb(Pb_{0.31}Zr_{0.28}Ti_{0.41})O_3$ thin films deposited by multi-target reactive sputtering onto platinized silicon wafers.

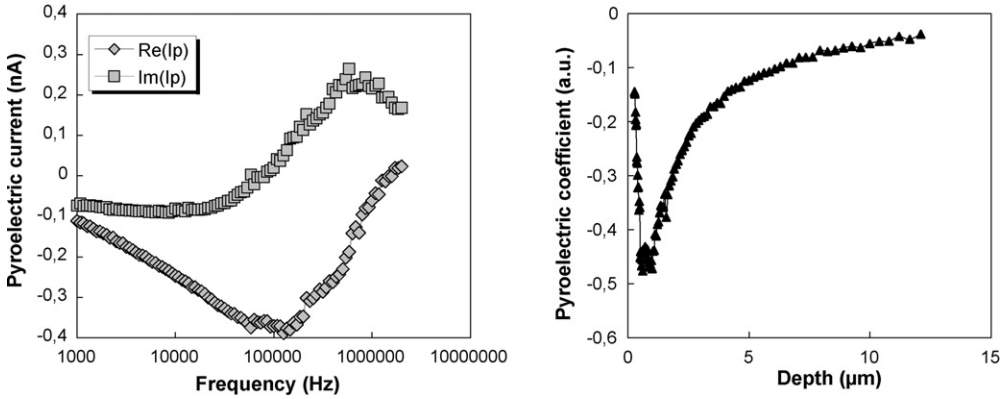

Fig. 2. Pyroelectric current spectrum (a) and pyroelectric coefficient profile (b) of a functional gradient ceramic $BaTi_{1-x}Sn_xO_3$ with $0.075 \leq x \leq 0.15$ at the $x = 0.075$ side.

the top electrode, the polarization direction has changed and the averaged pyroelectric coefficient increased up to 15 nC/cm^2 K. The positive values of polarization near the bottom electrode are caused by the presence of a space charge layer with a thickness of about 220 nm which is the origin of self-polarization.[20]

The pyroelectric current spectrum of a functional gradient ceramic $BaTi_{1-x}Sn_xO_3$ with $0.075 \leq x \leq 0.15$ is presented in Fig. 2a. A sufficient pyroelectric signal was obtained only for a sample where the poling dc voltage was applied to the Sn-poor side with $x = 0.075$. This is attributed to a Curie point below room temperature at the Sn-rich side.[18] The pyroelectric coefficient profile (Fig. 2b) was evaluated using the near surface approximation from Eq. (5).

Fig. 3 shows the pyroelectric coefficient profile of undoped and doped SBN crystals derived from the pyroelectric response to rectangular modulated IR light using Eq. (7). Undoped SBN crystals exhibit a strong depolarization effect after alternating electric field treatment (AEFT). In the case of Cr or Ce doping no depolarization was obtained. This is attributed to the well known in this case domain wall pinning.[19] The different behavior of Cr and Ce is due to different lattice sites, Cr substitutes Nb and Ce both Sr and Ba. Obviously, space charges appear in the latter case[19] which can give an explanation of the increase in pyroelectric response.

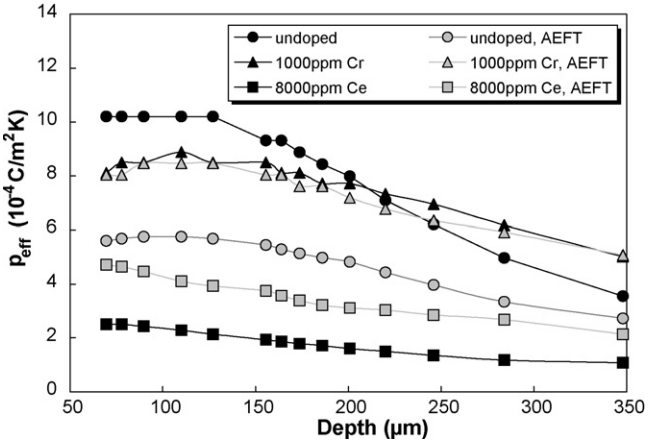

Fig. 3. Pyroelectric coefficient profiles of undoped and doped SNB crystals before and after alternating electric field treatment (AEFT).

4. Conclusions

The application of thermal wave techniques to the evaluation of the pyroelectric polarization distribution in ferroelectrics was demonstrated. For thermally semi-infinite samples, harmonic waves are suitable to determine the polarization profile near the surface. Low frequency square waves yield approximate values

at of the penetration depth of the fundamental wave.

Acknowledgements

This work was supported by the Herbert-Quandt/ALTANA Foundation and by the German Research Council (Deutsche Forschungsgemeinschaft) as part of the Research Group FOR520. The authors thank Prof. S. Kapphan (University of Osnabrück, Germany) and Dr. R. Steinhausen (Martin Luther University Halle, Germany) for providing samples.

References

1. Chynoweth, A. G., Dynamic method for measuring the pyroelectric effect with special reference to barium titanate. *J. Appl. Phys.*, 1956, **27**, 78–84.
2. Glass, A. M., Dielectric, thermal, and pyroelectric properties of ferroelectric $LiTaO_3$. *Phys. Rev. B*, 1968, **172**, 564–571.
3. Liu, S. T., Heaps, J. D. and Tufte, O. N., The pyroelectric properties of the lanthanum-doped ferroelectric PLZT ceramics. *Ferroelectrics*, 1972, **3**, 281–285.
4. Petersen, R. L., Day, G. W., Gruzensky, P. M. and Phelan, R. J., Analysis of response of pyroelectric optical detectors. *J. Appl. Phys.*, 1974, **45**, 3296–3303.
5. Lang, S. B. and Das Gupta, D. K., A technique for determination the polarization distribution in thin polymer electrets using periodic heating. *Ferroelectrics*, 1981, **39**, 1249–1252.
6. Bezdetny, N. M., Zeinally, A. Kh. and Khutorsky, V. E., Investigation of the polarization distribution in ferroelectrics by a dynamic pyro-effect method. *Izv. AN SSSR, Ser Fiz.*, 1984, **48**, 200–203 (in Russian).
7. Zajos, H. J., Spatial temperature and bound-charge distribution in tetragonal ferroelectrics irradiated by laser pulses. *Infrared Phys.*, 1980, **20**, 203–213.
8. Lang, S. B. and Das-Gupta, D. K., Laser-intensity-modulation method: a technique for determination of spatial distributions of polarization and space charge in polymer electrets. *J. Appl. Phys.*, 1986, **59**, 2151–2160.
9. Ploss, B., Emmerich, R. and Bauer, S., Thermal wave probing of pyroelectric distributions in the surface region of ferroelectric materials: a new method of analysis. *J. Appl. Phys.*, 1992, **72**, 5363–5370.
10. Bauer, S. and Bauer-Gogonea, S., Current practice in space charge and polarization profile measurements using thermal techniques. *IEEE Trans. Dielectr. Electr. Insul.*, 2003, **10**, 883–902.
11. Sandner, T., Suchaneck, G., Koehler, R., Suchaneck, A. and Gerlach, G., High frequency LIMM—a powerful tool for ferroelectric thin film characterization. *Integr. Ferroelectr.*, 2002, **46**, 243–257.
12. Carslaw, H. S. and Jaeger, J. C., *Conduction of Heat in Solids*. Clarendon, Oxford, 1959.
13. Lang, S. B., An analysis of the integral equation of the surface laser intensity modulation method using the constrained regularization method. *IEEE Trans. Dielectr. Electr. Insul.*, 1998, **5**, 70–76.
14. Lang, S. B., Laser intensity modulation method (LIMM): review of the fundamentals and a new method for data analysis. *IEEE Trans. Dielectr. Electr. Insul.*, 2004, **11**, 123–902.
15. Malyshkina, O. V. and Movchikova, A. A., Calculation of the coordinate dependences of the effective pyroelectric coefficient under conditions of rectangular heat flux modulation with the use of digital methods for signal processing. *Fiz. Tverdogo Tela*, 2006, **48**, 965–966 (in Russian).
16. Suchaneck, G., Lin, W.-M., Vidyarthi, V. S., Gerlach, G. and Hartung, J., Perspectives of large area $Pb(Zr,Ti)O_3$ thin film deposition. *J. Europ. Ceram. Soc.*, 2007, **27**, 3789–3792.
17. Steinhausen, R., Langhammer, H. Th., Kouvatov, A. Z., Pientschke, C., Beige, H. and Abicht, H.-P., Bending actuators based on monolithic barium-titanate-stannate ceramics as functional gradient materials. *Mater. Sci. Forum*, 2005, **494**, 167–174.
18. Smolenskii, G. A. and Isupov, V. A., Ferroelectric properties of solid solution of barium stannate in barium titanate. *Zh. Tekhn. Fiz.*, 1954, **24**, 1375–1386 (in Russian).
19. Lehnen, P., Kleeman, W., Woike, Th. and Pankrath, R., Ferroelectric nanodomains in the uniaxial relaxor system SBN. *Phys. Rev.*, 2001, **B64**, 224109.
20. Lu, X., Schlaphof, F., Grafström, S., Loppacher, Ch., Eng, L. M., Suchaneck, G. *et al.*, Scanning force microscopy investigation of the $Pb(Zr_{0.25}Ti_{0.75})O_3$/Pt interface. *Appl. Phys. Lett.*, 2002, **81**, 3215–3217.